Environ Sci Technol. Author manuscript; available in PMC Jul 1, 2012. PMC
Published in final edited form as: NIHMSI
Environ Sci Technol. Jul 1, 2011; 45(13): 5564–5571.
Published online Jun 1, 2011. doi: 10.1021/es200157h

Aggregation Kinetics of Citrate and Polyvinylpyrrolidone Coated Silver Na in Monovalent and Divalent Electrolyte Solutions

Khanh An Huynh and Kai Loon Chen*

Department of Geography and Environmental Engineering, Johns Hopkins University, Baltimore, Maryland 21218-2686
* Corresponding author: Kai Loon Chen, Email: kailoon.chen@jhu.edu, Phone: (410) 516-7095

Abstract

The aggregation kinetics of silver nanoparticles (AgNPs) that were coated with two commonly use agents—citrate and polyvinylpyrrolidone (PVP)—were investigated. Time-resolved dynamic light (DLS) was employed to measure the aggregation kinetics of the AgNPs over a range of monovaler electrolyte concentrations. The aggregation behavior of citrate-coated AgNPs in NaCl was in excel with the predictions based on Derjaguin–Landau–Verwey–Overbeek (DLVO) theory, and the Ham of citrate-coated AgNPs in aqueous solutions was derived to be 3.7 × 10^{-20} J. Divalent electrolytes efficient in destabilizing the citrate-coated AgNPs, as indicated by the considerably lower critical c concentrations (2.1 mM $CaCl_2$ and 2.7 mM $MgCl_2$ vs. 47.6 mM NaCl). The PVP-coated AgNPs w significantly more stable than citrate-coated AgNPs in both NaCl and $CaCl_2$, which is likely due tc repulsion imparted by the large, non-charged polymers. The addition of humic acid resulted in the the macromolecules on both citrate- and PVP-coated AgNPs. The adsorption of humic acid induce electrosteric repulsion that elevated the stability of both nanoparticles in suspensions containing N concentrations of $CaCl_2$. Conversely, enhanced aggregation occurred for both nanoparticles at hig concentrations due to interparticle bridging by humic acid clusters.

Introduction

Because of the optical and antimicrobial properties and electrical conductivity of silver nanoparticl 4), these nanomaterials are already finding applications in a wide variety of fields, which includes chemical, and electrical engineering. The combination of their antimicrobial activity and relative l likely the key reason for nanosilver-containing products to presently comprise more than 50% of t consumer products that contain engineered nanoparticles (5). For example, AgNPs are being incor clothes, bandages, and food containers as deodorizers and disinfectants (6). In addition, studies hav conducted to explore the use of AgNPs for drinking water treatment applications (7).

With AgNPs increasingly being manufactured and utilized in consumer products, AgNPs are likel into surface waters and the subsurface. Recent studies have shown that AgNPs can exert toxic effe mammalian cells (8, 9) and microorganisms (4, 10), even though the mechanisms for cytotoxicity well understood. Thus, the potential release of these engineered nanomaterials into the environme concerns on their impacts on the ecosystem and human health.

Currently, the most commonly used method to synthesize spherical, reasonably monodisperse Ag reduction of silver salts (3). In addition, AgNPs are often modified with capping agents. Since thes agents are usually negatively charged species or relatively large, hydrophilic polymers, the adsorpt agents will impart colloidal stability to AgNPs by either enhancing their surface charge or introduc electrosteric repulsion (11). This enhancement in colloidal stability is especially critical for applica require the dispersion of AgNPs in aqueous solutions, such as the high ionic strength solutions typ encountered in biomedical applications.

The environmental impact of AgNPs is greatly dependent on their mobility and aggregation behav natural and engineered environment. Recently, Li et al. (12) investigated the influence of solution the aggregation kinetics of unmodified AgNPs and obtained the critical coagulation concentrations these nanoparticles through time-resolved dynamic light scattering (DLS). Since the CCC represen minimum amount of electrolyte needed to completely destabilize the suspension (13), it provides a of colloidal stability for AgNPs and hence can be used to in the prediction of the fate and transport natural and engineered systems. To date, no study has been conducted to derive the CCCs of AgN been modified with capping agents. Furthermore, the impact of natural organic matter (NOM), wh ubiquitous in aquatic systems, on the colloidal stability of modified AgNPs is still not well underst

The objective of this study is to quantify and compare the aggregation kinetics and colloidal stabil that were synthesized through the reduction of a Tollens' reagent and modified with two common agents—citrate and polyvinylpyrrolidone (PVP). Time-resolved DLS measurements were conduct aggregation kinetics of both modified AgNPs over a range of monovalent (NaCl) and divalent (M electrolyte concentrations. The Derjaguin–Landau–Verwey–Overbeek (DLVO) theory was used t experimental data in order to derive the Hamaker constant of citrate-coated AgNPs. In addition, th humic acid on the colloidal stability of both citrate- and PVP-coated AgNPs was investigated.

Materials and Methods

Silver Nanoparticle Synthesis and Characterization

All reagents used for the preparation of the citrate- and PVP-coated AgNPs were purchased from Unmodified AgNPs were first synthesized through the reduction of a Tollens' reaction using gluco Details for the preparation of the unmodified AgNP suspension are provided in the Supporting Inf This suspension will be referred to as the *original AgNP stock suspension*. Measurements using in coupled plasma mass spectroscopy (ICP-MS) showed that the total and dissolved silver concentrat freshly prepared stock suspension were 10.360 mg/L and 0.002 mg/L, respectively. These measure indicated that the yield of AgNP formation was nearly 100%.

The *citrate-coated* and *PVP-coated AgNP stock suspensions* used in this study were prepared by cl
original AgNP stock suspension and re-suspending the nanoparticles in citrate and PVP solutions.
preparation of these stock suspensions are provided in the SI. According to the supplier (Sigma), tl
coat the AgNPs has an average MW of 10 kDa. The stock suspensions were contained in tightly ca
glass bottles and stored in the dark at 4°C. Through ICP-MS analysis, the AgNP and dissolved silv
concentrations in the citrate-coated AgNP stock suspension used for the aggregation experiments v
determined to be 8.467 mg/L and 0.112 mg/L, respectively. The AgNP and dissolved silver concer
PVP-coated AgNP stock suspension used for the aggregation experiments were 8.247 mg/L and 0.
respectively. The total citrate and PVP concentrations in the citrate- and PVP-coated AgNP stock s
were 1 μM and 6.6 mg/L total organic carbon (TOC), respectively.

The absorbance spectra of citrate-and PVP-coated AgNP suspensions were obtained over a range c
from 300 to 900 nm by using a UV-Vis spectrophotometer (UV-1800, Shimadzu). In addition, the
PVP-coated AgNPs were examined using a transmission electron microscope (TEM) (Philips CM
drop of AgNP stock suspension was deposited and dried on a specimen copper TEM grid, which w
a Lacey carbon film (SPI Supplies, PA), before being observed under the TEM at 300 kV. The ele
composition and crystalline structure of the AgNPs were obtained through energy dispersive X-ray
(EDS) and selected area electron diffraction (SAED) analysis, respectively, with the employment c
The electron diffraction pattern of PVP-coated AgNPs was obtained by using a Philips EM 420 TE

Determination of Silver Nanoparticle and Dissolved Silver Concentrations

The AgNP and dissolved silver concentrations of the AgNP stock and diluted suspensions used in
obtained through centrifugal ultrafiltration (using 3-kDa centrifugal membrane filters) and ICP-MS
provided in the SI.

Solution Chemistry

ACS-grade electrolyte (NaCl, $CaCl_2$, and $MgCl_2$) stock solutions were prepared and filtered using
alumina syringe filters (Anotop 25, Whatman) before use. Humic acid stock solution was prepared
Suwannee River humic acid (Standard II, International Humic Substances Society) in DI water. De
provided in the SI. All experiments and measurements were performed at pH 7.0 ± 0.1 (buffered w
$NaHCO_3$).

Electrophoretic Mobility Measurements

A ZetaPALS analyzer (Brookhaven, NY) was used to measure the electrophoretic mobilities (EPM
and PVP-coated AgNPs over a range of electrolyte concentrations at 25°C. For each solution chem
measurements were conducted for each of at least 3 samples. The zeta (ζ) potentials were convert
average EPMs by using the tabulated values that were provided by Ottewill and Shaw (15).

Time-Resolved Dynamic Light Scattering

Time-resolved DLS measurements of aggregating AgNP suspensions were performed using a light
unit. This unit comprises an argon laser (Lexel 95, Cambridge laser, CA) with a wavelength of 48
photomultiplier tube mounted on a goniometer (BI-200SM, Brookhaven, NY), a digital correlator
Brookhaven, NY), and a thermostated vat filled with an index-matching *cis*- and *trans*-mixture of
decahydronaphthalene which was maintained at 25°C for all our measurements. The detailed proce

DLS measurements is provided in the SI. For all aggregation experiments, the AgNP suspensions u measurements had a total volume of 1 mL and a AgNP concentration of 1.129 mg/L of citrate-coat 1.010 mg/L of PVP-coated AgNPs (7.5 times dilution from citrate- or PVP-coated AgNP stock sus respectively). The total citrate and PVP concentrations of the final citrate- and PVP-coated AgNP s were 0.13 μM and 0.88 mg/L TOC, respectively.

All DLS measurements were conducted at a scattering angle of 90°. Each autocorrelation function accumulated over 15 s and the intensity-weighted hydrodynamic diameter was then derived using s cumulant analysis (Brookhaven software). Time-resolved DLS measurements were performed ove of between 12 min and 3 h in order to achieve a large enough increase in hydrodynamic diameter f derivation of aggregation kinetics.

Determination of Aggregation Kinetics

The early-stage aggregation kinetics of AgNPs can be obtained from the initial rate of change of hy diameter, D_h, with time, t, as measured by time-resolved DLS. In the early aggregation stage, the in aggregation rate constant, k, is proportional to the initial rate of increase in D_h and inversely propo initial primary AgNP concentration in the suspension, N_0 (16, 17):

k∝1N0(dDh(t)dt)t→0

A linear least squares regression analysis of the initial increase in D_h was conducted to obtain k. Fo chemistries, this analysis was performed over the time period in which the hydrodynamic diameter 1.3 times of the initial hydrodynamic diameter, $D_{h,0}$. At low electrolyte concentrations, however, th hydrodynamic diameter failed to reach 1.3 $D_{h,0}$. Under such conditions, the linear regression was p a prolonged time period (> 90 min). For all solution chemistries, the y-intercept of the fitted line di nm in excess of $D_{h,0}$.

The attachment efficiency, α, is used to quantify the aggregation kinetics of AgNPs. It is calculatec normalizing the aggregation rate constant obtained in the solution of interest to the rate constant ob favorable (non-repulsive) aggregation conditions, k_{fast} (16-18):

α=kkfast=1N0(dDh(t)dt)t→01(N0)fast(dDh(t)dt)t→0,fast

The terms with subscript "fast" refer to favorable conditions. To calculate α in the presence of hum was determined using (dDh(t)dt)t→0,fast obtained for the same type of AgNPs in the *absence* of h the same electrolyte of interest. In such cases, α values exceeding unity indicates that interparticle taking place (19).

Detection of AgNP Dissolution

The degree of nanoparticle dissolution taking place in our systems was determined since dissolutio influence the mechanism of AgNP aggregation. Specifically, the precipitation of AgCl resulting fro in Ag^+ concentration due to the dissolution of AgNPs may lead to interparticle bridging between A will in turn enhance the nanoparticle aggregation kinetics (12). In this study, dissolution experimen conducted by measuring the dissolved silver concentrations of the citrate- and PVP-coated AgNP s prepared at the highest electrolyte concentrations which were used for the aggregation experiments measurements were conducted using ICP-MS and the details are provided in the SI.

Results and Discussion

Physicochemical Properties of Citrate- and PVP-Coated AgNPs

The size distribution of the citrate-coated AgNPs (Figure 1a) was determined by using the Digital I software (Gatan, CA) to measure the diameters of 210 nanoparticles randomly selected from a TEI representative TEM image of the AgNPs is presented in the insert. The nanoparticles were observe spherical with slight angular features. The number average diameter of the citrate-coated AgNPs w the standard deviation was 18.9 nm. Through 20 DLS measurements, the average intensity-weight hydrodynamic diameter of stable citrate-coated AgNPs prepared in DI water was determined to be which is very similar to the number average diameter of the nanoparticles. The average intensity-w hydrodynamic diameter of PVP-coated AgNPs obtained from 20 DLS measurements was 66.9 nm.

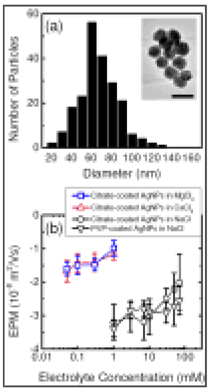

FIGURE 1

(a) Size distribution of 210 citrate-coated AgNPs. The inset presents a representative TEM image of the citrate-coated AgNPs. The scale bar represents 100 nm. (b) Electrophoretic mobilities (EPMs) of citrate- and PVP-coated AgNPs as a function of electrolyte **...**

Absorbance peaks for citrate- and PVP-coated AgNP suspensions were at 431 nm and 418 nm, res (Figure S1 in SI). These values are within the reported range for AgNPs with the size of 57–87 nm resolution TEM imaging of both AgNPs revealed lattice fringes with different alignments within a nanoparticle, which are indicative of the polycrystalline nature of AgNPs synthesized through the method (Figure S2).

SAED analysis was performed on citrate- and PVP-coated AgNP clusters and the distances betwee planes (d-spacing) were determined by measuring the diameters of the first four rings on the diffra (Figure S3a and Figure S4a). The similarity in the first four d-spacing values between the AgNPs (1.42 Å, 1.23 Å for citrate-coated AgNPs and 2.40 Å, 2.08 Å, 1.50 Å, 1.23 Å for PVP-coated AgNI metal (2.36 Å, 2.04 Å, 1.44 Å, 1.23 Å (21)) confirmed that the nanoparticles have the same crystal as bulk silver.

The elements and their relative abundance of citrate- and PVP-coated AgNPs were obtained by pe EDS on AgNP samples which were freshly dried on TEM grids. The EDS spectra of randomly sele and PVP-coated AgNP clusters (Figure S3b and Figure S4b) showed that the nanoparticles were m composed of silver and the amount of oxygen of the whole cluster was relatively small. Therefore, from both SAED and EDS analyses confirmed that our synthesis method resulted in the productior AgNPs.

Electrokinetic Properties of Citrate- and PVP-Coated AgNPs

Figure 1b presents the EPMs of citrate-coated AgNPs measured over a range of monovalent (NaCl ($CaCl_2$ and $MgCl_2$) electrolyte concentrations. The measurements showed that citrate-coated AgNI negatively charged over the entire range of monovalent and divalent electrolyte concentrations use Since the pK_a values of citric acid are 3.13, 4.72, and 6.33 (22), the carboxylic acid groups of citrat are mostly deprotonated at pH 7 and will thus contribute to the surface charge of citrate-coated Ag addition, the residual side products from AgNP synthesis could also contribute to the negative surf these nanoparticles. With increasing electrolyte concentrations, the EPMs of citrate-coated AgNPs negative due to an increase in charge screening (for NaCl) or charge neutralization (for $CaCl_2$ and

Figure 1b also presents the EPMs of PVP-coated AgNPs over a range of NaCl concentrations. It w that PVP-coated AgNPs had similar EPMs as citrate-coated AgNPs. Since PVP polymers are neutr PVP concentration in the suspension was relatively low (0.88 mg/L TOC), the AgNPs may not be coated with PVP and the negative surface charge is likely due to the residual side products which v on the nanoparticle surface.

Dissolution of Citrate- and PVP-Coated AgNPs at High Electrolyte Concentrations

Because the precipitation of silver salts may enhance the aggregation kinetics of AgNPs, we perfo dissolution experiments at the highest electrolyte concentrations that were used in our aggregation establish the dissolved silver concentrations under these solution chemistries. These dissolution ex performed at 455 mM NaCl, 27 mM $CaCl_2$, and 27 mM $MgCl_2$ for citrate-coated AgNPs and at 45 and 27 mM $CaCl_2$ for PVP-coated AgNPs. These are the electrolyte concentrations at which the na underwent diffusion-limited aggregation (to be discussed in the following section). Control experi performed in the absence of electrolytes. For these experiments, the samples were prepared in the s for the DLS experiments by diluting the citrate- or PVP-coated AgNP stock suspension 7.5 times b addition of either the electrolyte solution of interest or DI water (for control experiments).

The dissolved silver concentrations of the citrate- and PVP-coated AgNP suspensions prepared in electrolyte solutions are presented in Figure 2. It should be noted that the initial AgNP and dissolv concentrations of citrate- and PVP-coated AgNP suspensions were different because the citrate- an AgNP stock suspensions were prepared separately. The slight increase in dissolved silver concentr citrate- and PVP-coated AgNP suspensions prepared in DI water after 30 min indicated that some have occurred. The increase in temperature (from 4 to 25°C) and dissolved oxygen concentration, decrease in citrate and PVP concentrations, are expected to lead to the slight dissolution of both A diluted in DI water (23-25).

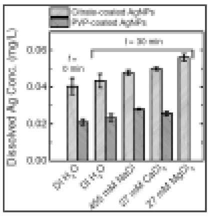

FIGURE 2

Dissolved silver concentrations at either 0 or 30 min after the preparation of citrate- and PVP-coated AgNP suspensions in different solution chemistries at pH 7.0. The initial AgNP concentrations of the citrate- and PVP-coated AgNP suspensions (at *t* ...

Also shown in Figure 2, citrate- and PVP-coated AgNPs were generally observed to undergo a hig dissolution in all electrolyte solutions than in DI water. These results are consistent to other observ increase in ionic strength can enhance AgNP dissolution (12). The presence of chloride ions in the solutions will lead to the formation of soluble silver chloride complexes, such as $AgCl_2^-$ and AgCl can accelerate the dissolution of AgNPs. The measured dissolved silver concentrations in solutions NaCl, 27 mM $CaCl_2$, and 27 mM $MgCl_2$ were used as input parameters for the conservative estima concentrations of dissolved silver species in our aggregation experiments at the same solution cher MINTEQ, Version 3.0). Due to the considerably low dissolved silver concentrations, the simulatio that no precipitation of any silver species (including AgCl) would occur at equilibrium. This result the minor dissolution of either citrate- or PVP-coated AgNPs in our systems did not lead to precipi interparticle bridging of AgNPs over the range of NaCl, $CaCl_2$, and $MgCl_2$ concentrations employe

Aggregation Kinetics of Citrate-Coated AgNPs in Monovalent Electrolyte Solution

The attachment efficiencies of citrate-coated AgNPs are presented as a function of NaCl concentra Figure 3a. Representative aggregation profiles are presented in Figure S5. The aggregation behavic coated AgNPs in NaCl solutions is consistent with the DLVO theory. At low concentrations of Na in NaCl concentration will elevate the degree of charge screening and hence allow for an increase i kinetics, as reflected by the rise in attachment efficiency. This regime is known as the reaction-lim < 1). At high NaCl concentrations, the charge of citrate-coated AgNPs is completely screened and barrier between AgNPs is eliminated. Under such conditions, the nanoparticles undergo diffusion-l aggregation ($\alpha = 1$). In the diffusion-limited regime, the kinetics of aggregation has reached a maxi independent of the NaCl concentration. The CCC, which delineates the reaction- and diffusion-lim was derived by determining the intersection of the extrapolations through both regimes (17). In Na the CCC of citrate-coated AgNPs was 47.6 mM.

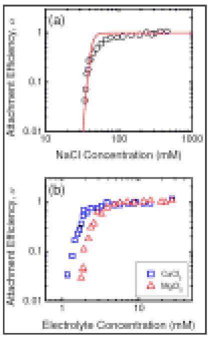

FIGURE 3

Attachment efficiencies of citrate-coated AgNPs as functions of (a) NaCl and (b) $CaCl_2$ and $MgCl_2$ concentrations at pH 7.0. The solid line in a represents DLVO prediction using a Hamaker constant of 3.7×10^{-20} J. For all experiments, the citrate **...**

Recently, Li et al. (12) employed time-resolved DLS to investigate the aggregation kinetics of unn that were synthesized through the reduction of a Tollens' reagent using D-maltose. In their study, s AgNP dissolution appeared to have taken place concurrently with nanoparticle aggregation. Li and detected an immediate and drastic decrease in hydrodynamic diameter (up to 50% decrease) when stock solutions (NaCl, $NaNO_3$, or $CaCl_2$) were introduced into the AgNP suspensions. Through TE they also observed interconnected AgNPs within AgNP aggregates which were formed in the prese which they attributed to interparticle bridging by AgCl precipitates (12). In contrast, the degree of the citrate- and PVP-coated AgNPs used in this study was too low to result in AgCl precipitation. considerably higher degree of nanoparticle dissolution in Li et al.'s study (12) is possibly due to th capping agent in their systems. In addition, citrate can serve as a reducing agent which will inhibit dissolution of the citrate-coated AgNPs in our study. Hence, a comparison of the aggregation beha in both studies demonstrates that both the methods for nanoparticle preparation and presence of ca have significant impacts on the colloidal stability and mechanisms of aggregation of AgNPs.

Comparing Citrate-Coated AgNP Aggregation Kinetics with DLVO Theory

The aggregation kinetics of citrate-coated AgNPs obtained through time-resolved DLS was compa DLVO theory. The attachment efficiency of aggregating spherical colloidal particles can be calcul the following expression which accounts for colloidal and hydrodynamic interactions (17, 26)

$$\alpha=\int0\infty\beta(h)\exp[VA(h)/(kT)](2a+h)2dh\int0\infty\beta(h)\exp[VT(h)/(kT)](2a+h)2dh$$

where h is the separation distance between two particles, a is the particle radius (35.65 nm, based c average diameter of the citrate-coated AgNPs), k is the Boltzmann constant, and T is the absolute t (298.15 K). The van der Waals attraction, $V_A(h)$, was calculated using the expression proposed by that accounts for the electromagnetic retardation effect. The total interaction energy between two p is the sum of the van der Waals attraction, $V_A(h)$, and electrical double layer interaction, $V_R(h)$. Th superposition approximation expression was used to calculate the electrical double layer interactio function $\beta(h)$ is used to correct for the hydrodynamic interactions between two approaching particl Details on the calculation of DLVO interactions can be found in the SI.

In this study, ζ potentials, which were converted from the EPMs, were used instead of surface pote calculation of $V_R(h)$ (30). Logarithmic regression analysis was performed on the ζ potentials to der relationship between ζ potential and NaCl concentration. This relationship was then used for the ca (h). Using the Hamaker constant for citrate-coated AgNPs in aqueous solutions, which is part of th for $V_A(h)$, as the single fitting parameter, the experimentally obtained attachment efficiencies were theoretical calculations for attachment efficiencies (eq 3).

The solid line in Figure 3a represents the best-fitting theoretical attachment efficiencies derived us constant of 3.7×10^{-20} J for citrate-coated AgNPs in aqueous solutions. This value falls within the $(2.9 \pm 0.8) \times 10^{-20}$ J suggested by Fornasiero and Grieser (31). Furthermore, Figure 3a shows that t experimentally obtained attachment efficiencies are in remarkable agreement with DLVO predictic key assumptions of DLVO theory is that the charge on the particle surface is uniformly distributed Previously, discrepancies between experimental results and theoretical predictions had been observ types of particles and these discrepancies were attributed to the heterogeneity of surface charge (3(the good agreement between the experimental results and theoretical prediction in this study may b of a uniform charge distribution on the citrate-coated AgNP surface.

Aggregation Kinetics of Citrate-Coated AgNPs in Divalent Electrolyte Solutions

The aggregation kinetics of citrate-coated AgNPs in $CaCl_2$ and $MgCl_2$ electrolytes are presented in Similar to the inverse stability profile obtained in the presence of NaCl (Figure 3a), the presence o and diffusion-limited regimes showed that the aggregation kinetics of citrate-coated AgNPs in Ca(electrolytes are controlled by electrostatic interactions. The CCCs of citrate-coated AgNPs in the p $CaCl_2$ and $MgCl_2$ were 2.1 mM and 2.7 mM, respectively. These values are much smaller than the in NaCl, since Ca^{2+} and Mg^{2+} ions can neutralize the surface charge of citrate-coated AgNPs throu interactions with the carboxyl groups of the adsorbed citrate molecules. The results from the aggre experiments corroborate with the EPM measurements which showed that mobilities of citrate-coat nanoparticles were considerably less negative in the presence of $CaCl_2$ and $MgCl_2$ than in NaCl (F addition, the CCC of citrate-coated AgNPs in $CaCl_2$ is lower than that in $MgCl_2$. This disparity in (due to Ca^{2+} ions having a higher propensity to form complexes with citrate compared with Mg^{2+} ic

from the higher stability constant of monodentate Ca-citrate complexes compared to monodentate
complexes at 0 mM ionic strength and 25°C ($10^{1.4}$ vs. $10^{1.0}$) (32). Therefore, Ca^{2+} ions are expecte
efficient than Mg^{2+} ions in neutralizing the surface charge of citrate-coated AgNPs.

Comparing Aggregation Kinetics of PVP-Coated AgNPs with Citrate-Coated AgNPs

Figure 4 presents the inverse stability profiles of PVP- and citrate-coated AgNPs in NaCl and CaC
The total PVP concentration in the PVP-coated AgNP suspensions was 0.88 mg/L TOC, which is
equivalent to 0.14 µM PVP by using a PVP MW of 10 kDa. Therefore, the molar concentration of
suspensions is comparable to that of citrate in the citrate-coated AgNP suspensions (0.13 µM). Wh
concentrations of capping agents were used, the PVP-coated AgNPs were more stable than citrate-
in both electrolytes, as indicated by the considerably higher CCCs of PVP-coated AgNPs. In the p
NaCl, the CCC of PVP-coated AgNPs was 111.5 mM, compared to 47.6 mM for the citrate-coated
presence of $CaCl_2$, the CCCs of PVP- and citrate-coated AgNPs were 4.9 mM and 2.1 mM, respec

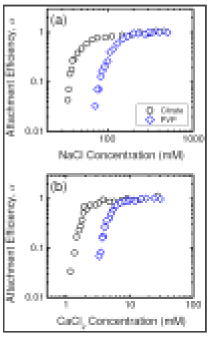

FIGURE 4

Attachment efficiencies of citrate- and PVP-coated AgNPs as functions of (a) NaCl and (b) $CaCl_2$ concentrations at pH 7.0. The attachment efficiencies of citrate-coated AgNPs in a and b are reproduced from Figures 3a and b, respectively. For citrate-coated **...**

Because PVP is an amphiphilic, non-charged polymer, the adsorption of PVP on AgNPs is likely
steric repulsion. Since the PVP concentration in the suspension was relatively low (0.88 mg/L TO
expected that the AgNPs were only partially coated with PVP. Thus, sufficient space was likely to
for PVP polymers to lie relatively flat on the nanoparticle surface with some polymer segments pr
the bulk solution (33). However, the existence of the reaction- and diffusion-limited regimes in the
stability profiles in both NaCl and $CaCl_2$ indicated that electrostatic interaction still played a signif
controlling the stability of PVP-coated AgNPs. Trace amount of residual side products from the A
process on the nanoparticle surface are likely the origin of the negative surface charge of the PVP-

At higher PVP concentrations, the PVP coverage will be increased and significant sections of adso
polymers will be expected to extend into the bulk solution (33), thus leading to steric repulsion to
major contributor to the stability of PVP-coated AgNPs. In the study of Badawy et al. (11), the stal
in PVP solutions with a concentration of 2,500 mg/L, which is much higher than that used in this s
investigated. The authors found that the ζ potential, which was close to neutral (ca. −7 mV), and hy
diameter of PVP-coated AgNPs remained constant over a wide range of pH conditions. Their obse
confirmed that steric repulsion was the dominant contributor to the high stability of the AgNPs and
contribution by electrostatic interactions was minor at elevated PVP concentrations.

Influence of Humic Acid on Aggregation Kinetics of Citrate- and PVP-Coated AgNPs

The aggregation kinetics of citrate-coated AgNPs in the absence and presence of humic acid are pr
functions of NaCl concentrations in Figure 5a. The presence of humic acid (1 mg/L TOC) increase
from 47.6 mM to 72.1 mM NaCl. The adsorption of humic acid macromolecules, which contains n

charged carboxyl groups, on the surface of citrate-coated AgNPs is very likely to result in electrost and thus increase the stability of the citrate-coated AgNPs. Although both citrate-coated AgNPs an are negatively charged at pH 7.0, humic acid may still adsorb on the modified nanoparticles throug interaction. It is also possible that the nanoparticles were not completely coated with citrate and th available surface sites for humic acid adsorption to take place.

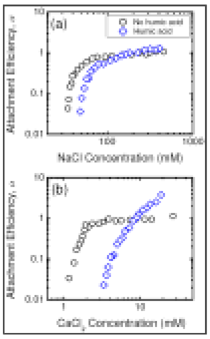

FIGURE 5

Attachment efficiencies of citrate-coated AgNPs in the absence and in the presence of humic acid (1 mg/L TOC) as functions of (a) NaCl and (b) $CaCl_2$ concentrations at pH 7.0. The attachment efficiencies of citrate-coated AgNPs in the absence of humic **...**

The aggregation behavior of citrate-coated AgNPs in the presence of humic acid and $CaCl_2$ is dissi in NaCl, as shown in Figure 5b. Specifically, no distinct reaction- and diffusion-limited regimes w the inverse stability profile. When the concentration of $CaCl_2$ was smaller than 9 mM, the citrate-c were more stable in the presence than in the absence of humic acid due to electrosteric stabilizatio concentrations above 9 mM, the attachment efficiencies were higher than unity and increased with $CaCl_2$ concentration. Similarly, enhanced aggregation of fullerene (19), gold (34), and silicon (35) was previously observed in the presence of humic acid at high $CaCl_2$ concentrations. Chen and Eli hypothesized that the enhanced aggregation was due to interparticle bridging of nanoparticles by h aggregates which were created from the complex formation between humic acid macromolecules a

PVP-coated AgNPs exhibited similar aggregation behavior in the presence of humic acid as that o AgNPs in both NaCl and $CaCl_2$ electrolytes (Figure S6). In NaCl solutions, the presence of humic the CCC of PVP-coated AgNPs from 111.5 mM to 155.1 mM. In the presence of $CaCl_2$, the PVP- were more stable in the presence than in the absence of humic acid below 18 mM. At $CaCl_2$ conce 18 mM, enhanced aggregation of PVP-coated AgNPs occurred in the presence of humic acid. How the highest $CaCl_2$ concentration employed (30 mM), the enhancement in aggregation kinetics of P AgNPs ($\alpha = 1.6$) was not as dramatic as that of citrate-coated AgNPs ($\alpha = 3.7$ at 19 mM $CaCl_2$). T enhancement in aggregation kinetics may be an indication that the adsorbed PVP can cause steric interparticle bridging by the humic acid clusters.

Environmental Implications

The aggregation kinetics of citrate-coated AgNPs is shown to be in excellent agreement with DLV Hamaker constant of citrate-coated AgNPs derived from this study is a critical parameter for the m prediction of the fate and transport of these nanoparticles in aquatic systems (36). PVP-coated Ag significantly more stable than citrate-coated AgNPs, likely due to the steric repulsion imparted by PVP molecules. Since the CCCs for both AgNPs are much higher than typical monovalent and div concentrations in freshwater systems, both AgNPs are expected to be highly mobile in these envir humic acid elevates the colloidal stability of both citrate- and PVP-coated AgNPs in NaCl and at l concentrations of $CaCl_2$, it enhances the aggregation kinetics at high $CaCl_2$ concentrations. Simila be conducted to establish the effects of other key components of NOM, such as fulvic acids and po on the aggregation kinetics of modified AgNPs. In addition, further research is required to assess tl reversibility of the adsorption of citrate and PVP on AgNPs, which will have important implicatior aggregation behavior and persistence of these nanoparticles in aquatic systems.

Supplementary Material

1_si_001

Click here to view.(469K, pdf)

Acknowledgments

K.A.H. was funded by the Vietnam Education Foundation and the Johns Hopkins University (JHU Center in Urban Environmental Health (P30ES03819). We acknowledge Dr. Kenneth Livi from th of Earth and Planetary Sciences (JHU) for performing the TEM, EDS, and SAED analyses of the /

Footnotes

Supporting Information Available

Additional figures and details for Materials and Methods and Results and Discussion are presented. This mate free of charge via the Internet at http://pubs.acs.org.

Literature Cited

1. McFarland AD, Van Duyne RP. Single silver nanoparticles as real-time optical sensors with zep sensitivity. Nano Lett. 2003;3(8):1057–1062.

2. Panáček A, Kvítek L, Prucek R, Kolár M, Večcřová R, Pizúrová N, Sharma VK, Nevěčná Tj, Zl colloid nanoparticles: synthesis, characterization, and their antibacterial activity. J Phys Chem B. 2 –16253. [PubMed]

3. Sharma VK, Yngard RA, Lin Y. Silver nanoparticles: green synthesis and their antimicrobial ac Advances in Colloid and Interface Science. 2009;145(1-2):83–96. [PubMed]

4. Sondi I, Salopek-Sondi B. Silver nanoparticles as antimicrobial agent: a case study on E-coli as Gram-negative bacteria. J Colloid Interf Sci. 2004;275(1):177–182. [PubMed]

5. The Project on Emerging Nanotechnologies. http://www.nanotechproject.org/inventories/consumer/analysis_draft/

6. Benn TM, Westerhoff P. Nanoparticle silver released into water from commercially available so Environ Sci Technol. 2008;42(11):4133–4139. [PubMed]

7. Li Q, Mahendra S, Lyon DY, Brunet L, Liga MV, Li D, Alvarez PJJ. Antimicrobial nanomateria disinfection and microbial control: Potential applications and implications. Water Research. 2008;4 4602. [PubMed]

8. AshaRani PV, Mun GLK, Hande MP, Valiyaveettil S. Cytotoxicity and Genotoxicity of Silver N Human Cells. ACS Nano. 2009;3(2):279–290. [PubMed]

9. Kim S, Choi JE, Choi J, Chung KH, Park K, Yi J, Ryu DY. Oxidative stress-dependent toxicity nanoparticles in human hepatoma cells. Toxicology in Vitro. 2009;23(6):1076–1084. [PubMed]

10. Choi O, Hu ZQ. Size dependent and reactive oxygen species related nanosilver toxicity to nitri Environ Sci Technol. 2008;42(12):4583–4588. [PubMed]

11. El Badawy AM, Luxton TP, Silva RG, Scheckel KG, Suidan MT, Tolaymat TM. Impact of En Conditions (pH, Ionic Strength, and Electrolyte Type) on the Surface Charge and Aggregation of S Nanoparticles Suspensions. Environ Sci Technol. 2010;44(4):1260–1266. [PubMed]

12. Li X, Lenhart JJ, Walker HW. Dissolution-Accompanied Aggregation Kinetics of Silver Nano Langmuir. 2010;26(22):16690–16698. [PubMed]

13. Chen KL, Smith BA, Ball WP, Fairbrother DH. Assessing the colloidal properties of engineere in water: case studies from fullerene C_{60} nanoparticles and carbon nanotubes. Environmental Chen (1):10–27.

14. Yin Y, Li Z-Y, Zhong Z, Gates B, Xia Y, Venkateswaran S. Synthesis and characterization of dispersions of silver nanoparticles through the Tollens process. J Matter Chem. 2002;12:552–527.

15. Ottewill RH, Shaw JN. Electrophoretic Studies On Polystyrene Latices. J Electroanal Chem. 1 –142.

16. Holthoff H, Egelhaaf S, Borkovec M, Schurtenberger P, Sticher H. Coagulation rate measurem colloidal particles by simultaneous static and dynamic light scattering. Langmuir. 1996;12(23):554

17. Chen KL, Elimelech M. Aggregation and Deposition Kinetics of Fullerene (C_{60}) Nanoparticles 2006;22(26):10994–11001. [PubMed]

18. Chen KL, Mylon SE, Elimelech M. Aggregation kinetics of alginate-coated hematite nanoparti monovalent and divalent electrolytes. Environ Sci Technol. 2006;40(5):1516–1523. [PubMed]

19. Chen KL, Elimelech M. Influence of humic acid on the aggregation kinetics of fullerene (C_{60}) in monovalent and divalent electrolyte solutions. J Colloid Interf Sci. 2007;309(1):126–134. [Pub

20. Kvítek L, Prucek R, Panáek A, Novotný R, Hrbáč J, Zbořil R. The influence of complexing ag concentration on particle size in the process of SERS active silver colloid synthesis. J Mater Chem –1105.

21. FIZ Karlsruhe. ICSD Web, Database #44387. http://icsd.fiz-karlsruhe.de/

22. Benjamin MM. Water Chemistry. Boston: McGraw-Hill; 2002.

23. Liu J, Sonshine DA, Shervani S, Hurt RH. Controlled release of biologically active silver from surfaces. ACS Nano. 2010;4(11):6903–13. [PMC free article] [PubMed]

24. Liu JY, Hurt RH. Ion Release Kinetics and Particle Persistence in Aqueous Nano-Silver Colloi Technol. 2010;44(6):2169–2175. [PubMed]

25. Kittler S, Greulich C, Diendorf J, Koller M, Epple M. Toxicity of Silver Nanoparticles Increas Storage Because of Slow Dissolution under Release of Silver Ions. Chemistry of Materials. 2010;2 4554.

26. McGown DNL, Parfitt GD. Improved Theoretical Calculation of Stability Ratio for Colloidal S
Journal of Physical Chemistry. 1967;71(2):449–&.

27. Gregory J. Approximate Expressions for Retarded van der Waals Interaction. Journal of Colloi
Science. 1981;83(1):138–145.

28. Gregory J. Interaction of Unequal Double-Layers at Constant Charge. Journal of Colloid and In
Science. 1975;51(1):44–51.

29. Honig EP, Roeberse Gj, Wiersema PH. Effect of Hydrodynamic Interaction on Coagulation Ra
Hydrophobic Colloids. Journal of Colloid and Interface Science. 1971;36(1):97–109.

30. Elimelech M, Gregory J, Jia X, Williams RA. Particle deposition and aggregation: measureme
and simulation. Butterworth-Heinemann: Oxford; Boston: 1995. p. xv.p. 441.

31. Fornasiero D, Grieser F. The Kinetics of Electrolyte Induced Aggregation of Carey Lea Silver
Colloid Interf Sci. 1991;141(1):168–179.

32. Martell AE, Smith RM, Motekaitis RJ. NIST Critically Selected Stability Constants of Metal C
Database. National Institute of Science and Technology; Gaithersburg, MD: 2004.

33. Robinson S, Williams PA. Inhibition of protein adsorption onto silica by polyvinylpyrrolidone.
2002;18(23):8743–8748.

34. Stankus DP, Lohse SE, Hutchison JE, Nason JA. Environ Sci Technol. ASAP; 2010. Interactio
Natural Organic Matter and Gold Nanoparticles Stabilized with Different Organic Capping Agents

35. Liu X, Wazne M, Chou T, Xiao R, Xu S. Influence of Ca^{2+} and Suwannee River Humic Acid c
of silicon nanoparticles in aqueous media. Water Research. 2011;45(1):105–112. [PubMed]

36. Petosa AR, Jaisi DP, Quevedo IR, Elimelech M, Tufenkji N. Aggregation and Deposition of E
Nanomaterials in Aquatic Environments: Role of Physicochemical Interactions. Environ Sci Techn
(17):6532–6549. [PubMed]